Chemical Science

EDGE ARTICLE

View Article Online
View Journal | View Issue

Cite this: *Chem. Sci.*, 2018, **9**, 8369

All publication charges for this article have been paid for by the Royal Society of Chemistry

Reductive cleavage of C=C bonds as a new strategy for turn-on dual fluorescence in effective sensing of H_2S†

Chunfei Wang,[a] Xiaoxiang Cheng,[a] Jingyun Tan,[a] Zhaoyang Ding,[a] Wenjing Wang,[b] Daqiang Yuan,[b] Gang Li,[a] Hongjie Zhang*[a] and Xuanjun Zhang*[a]

Received 2nd August 2018
Accepted 10th September 2018

DOI: 10.1039/c8sc03430c

rsc.li/chemical-science

Reductive cleavage of alkenes is rarely reported in synthetic chemistry. Here we report a unique H_2S-mediated reductive cleavage of C=C bonds under mild conditions, which is a successful new strategy for the design of probes for effective sensing of H_2S with turn-on dual-color fluorescence. A short series of phenothiazine ethylidene malononitrile derivatives were shown to react with H_2S, *via* reductive cleavage of C=C bonds with intramolecular cyclization reactions to form thiophene rings. Enlightened by this new reaction mechanism, four effective probes with turn-off to turn-on fluorescence switches were successfully applied for sensing H_2S, an important gaseous signalling molecule in living systems, among which PTZ-P4 exhibited two fluorescent colors after reductive cleavage. The dual-color probe was applied for imaging endogenous H_2S and showed distinct differences in brightness in living *C. elegans* for wild type N2, *glp-1* (*e2144*) mutants (higher levels of endogenous H_2S), and *cth-1* (*ok3319*) mutants (lower levels of endogenous H_2S). The discovery of H_2S-mediated reductive cleavage of C=C bonds is expected to be valuable for chemical synthesis, theoretical studies, and the design of new fluorescent H_2S probes.

Introduction

The discovery of novel reactivities with carbon–carbon double bonds (C=C) is not only useful for chemical synthesis and theoretical studies, but is also important for applications in biology, because C=C bonds are abundant in nature. As we all know, C=C bonds are fundamental structures of alkenes, where the C=C π bond is localized above and below the C–C σ bond wherein π electrons are relatively far away from the nuclei and are loosely bound, so that they can be easily attacked to construct a new bond.[1,2] Indeed, addition reactions are one of the common reactions of C=C bonds, such as reactions with HX (X = Cl, Br, I, OH, SH, RS, *etc.*) as described in Scheme 1a.[3] Additionally, C=C bonds can also be cleaved by oxidation as in the typical ozonolysis of alkenes (Scheme 1b).[4] However, because of their unique structure, reductive cleavage of alkenes (C_{sp^2}–C_{sp^2}) has rarely been reported so far.

In particular, the cleavage of C=C bonds in styrenes has been activated by a hard Lewis acid and ethanethiol.[5,6] In addition, Shi and coworkers reported reductive cleavage of C_{sp^2}–C_{sp^3} bonds using rhodium based catalysis.[7] In 2014, Bogdanov *et al.* reported that C=C bonds in 1,10-disubstituted isoindigos could be reductively cleaved by aqueous hydrazine hydrate.[8] In this work, we discovered an interesting H_2S-mediated reductive cleavage of C=C bonds under mild conditions.

As is well known, H_2S with sulfur at the lowest valence is an excellent reductant and nucleophile, found predominantly as HS^- at physiological pH and therefore displaying higher nucleophilicity compared with many other thiols in cells. Consequently, addition reactions have been a commonly used strategy for developing fluorescent H_2S probes in recent years. Highlighting the popularity and influence of this reaction mechanism, many fluorescent probes were well designed with rapid and specific responses to H_2S by disrupting the conjugated π-system of C=C bonds with addition reactions.[9–13] In addition, aryl nitro groups could be cleaved by thiolysis, triggering the fluorescence turn-on for the detection of H_2S or H_nS_n.[14–17] In the current work, we report our finding of H_2S-mediated reductive cleavage of C=C bonds under mild conditions (Scheme 1c), anticipated to be a new strategy for devising fluorescent H_2S probes. Concomitant with this has been the development of a dual-color fluorescent H_2S probe, which was successfully applied to monitor endogenous H_2S *in vivo*.

[a]*Faculty of Health Sciences, University of Macau, Macau SAR, China. E-mail: hjzhang@umac.mo; xuanjunzhang@umac.mo*

[b]*State Key Laboratory of Structural Chemistry, Fujian Institute of Research on the Structure of Matter, Chinese Academy of Sciences, Fuzhou 350002, China*

† Electronic supplementary information (ESI) available. CCDC 1846921 and 1846922. For ESI and crystallographic data in CIF or other electronic format see DOI: 10.1039/c8sc03430c

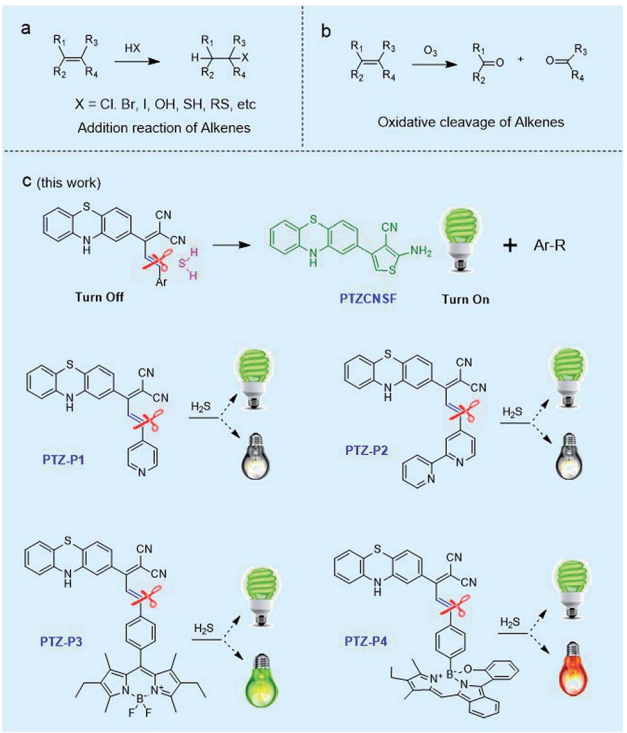

Scheme 1 (a) Typical addition reactions in alkenes. (b) Oxidative cleavage of alkenes by ozone. (c) Schematic representation of H_2S-mediated reductive cleavage of C=C bonds and four phenothiazine ethylidene malononitrile derivatives, with single- or dual-color turn-on fluorescence responses to H_2S.

Results and discussion

Design, synthesis and characterizations

Phenothiazine (PTZ), having a non-planar butterfly conformation, provides strong fluorescence, and has been used as an electron donor in photoelectric materials with a variety of applications.[18–22] We found that phenothiazine ethylidene malononitrile derivatives, **PTZ-P1**, **PTZ-P2**, **PTZ-P3** and **PTZ-P4**, could effectively react with H_2S *via* reductive cleavage of C=C bonds to yield a new fluorescent compound **PTZCNSF**.

Firstly, we use **PTZ-P1** as an example to discuss this novel reaction. PTZ is a strong electron donor whereas the dicyano group is a strong electron acceptor. The strong intramolecular charge transfer (ICT) in **PTZ-P1** gave rise to fluorescence quenching. Upon reacting with H_2S, **PTZ-P1** exhibited turn-on fluorescence with high selectivity and sensitivity.

To dissect the reaction mechanism, **PTZ-P1** was used to react with NaHS and the green fluorescent product, **PTZCNSF**, was successfully isolated. The NMR results of **PTZCNSF** (Fig. S25 and S26†) demonstrated the disappearance of the pyridine moiety and single crystal X-ray analysis was further used to confirm the structure. Single crystals of **PTZ-P1** and **PTZCNSF** for X-ray diffraction were obtained by slow evaporation of dichloromethane solutions, and ORTEP drawings are depicted in Fig. 1. During the transformation from **PTZ-P1** to **PTZCNSF**, C13, C14, C16 and C17 were connected by S2 from H_2S *via* an intramolecular cyclization reaction to yield **PTZCNSF**. It is

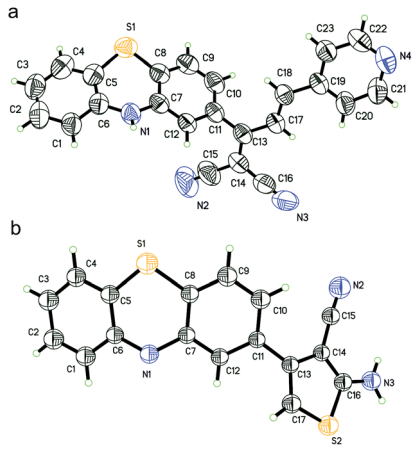

Fig. 1 ORTEP diagrams of **PTZ-P1** (a) and **PTZCNSF** (b) with ellipsoids adjusted to 50% probability. Solvent molecules were deleted for clarity.

surprising that the C17–C18 double bond in **PTZ-P1** was reductively cleaved and the pyridine moiety was cut off from the main structure, which was consistent with the NMR and MS analysis (Fig. 2a and b).

Three more derivatives, **PTZ-P2**, **PTZ-P3**, and **PTZ-P4**, were then designed and synthesized. For **PTZ-P3**, **BODIPY** was introduced for its good photostability, narrow emission, and high fluorescence quantum yield. In **PTZ-P4**, a red emitting

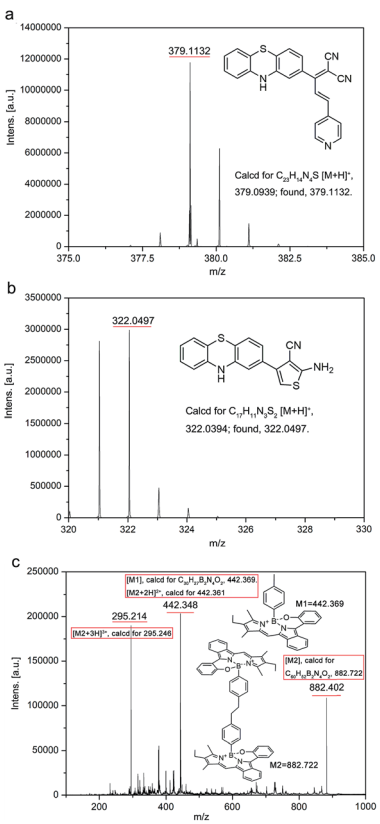

Fig. 2 MS data of **PTZ-P1**, **PTZCNSF**, and the red emitting products of **PTZ-P4** after the reaction with H_2S.

fluorophore (**BOBPY**) was chosen to conjugate with phenothiazine ethylidene malononitrile. **BOBPY** and derivatives were first developed by Jiao and coworkers,[23] and they are a kind of N_2O-type benzopyrromethene boron complex, wherein axial positions are substituted by corresponding boronic acids. We chose **BOBPY** here because of its excellent stability and high fluorescence quantum yield in different media. We hypothesized that both green and red emitting fluorophores will be released after reductive cleavage, and these could be used as dual-color fluorescent probes for sensing H_2S.

Detailed synthetic procedures are elucidated in the ESI.† Products and intermediates were fully characterized using ^1H NMR, ^{13}C NMR, HRMS and MALDI-TOF spectra (Fig. S8–S24, S27–S29†). All four derivatives could effectively react with H_2S *via* reductive cleavage of C=C bonds to produce **PTZCNSF**. However, pure single samples of the other part were difficult to isolate, because of the high reactivity of the $-CH_2$ moiety after reductive cleavage. Fortunately, the MALDI-TOF data of **PTZ-P4** revealed that the $-CH_2$ moiety could form R–CH_3 monomers and dimers (Fig. 2c) under these reductive conditions. Although the exact reaction pathway is still under investigation, MS, NMR, and single-crystal X-ray analysis undoubtedly confirmed this H_2S-mediated reductive cleavage of C=C bonds.

Absorption and fluorescence response of probes to H_2S

With these probes in hand, their responses to H_2S were studied. Initially, the absorption spectra of **PTZ-P1** upon addition of H_2S were assessed in PBS buffer (pH = 7.4)/DMSO (1/2, 2% v/v PEG 400) using aqueous NaHS as the H_2S source. As depicted in Fig. S5a†, **PTZ-P1** showed a main absorption peak at 330 nm along with a weak-intensity ICT band at around 500 nm. The absorption intensity decreased upon the gradual addition of H_2S (0–800 μM). However, **PTZ-P1** showed a turn-on fluorescence response at 488 nm with a 25-fold enhancement (Fig.-S5b†). The absorption and fluorescence of **PTZ-P2** responding to H_2S were similar to those of **PTZ-P1** (Fig. S6†). However, the increase of the fluorescence intensity was lower (only a 5-fold increase), which may be attributed to the stronger electron withdrawing strength of the dipyridyl moiety compared with the pyridyl group.

Subsequently, spectra titration experiments were performed to further investigate the response of **PTZ-P3** towards H_2S. The characteristic absorption peaks at 330 nm decreased upon gradual addition of H_2S (0–700 μM), whereas the peaks at 525 nm did not change much (Fig. 3a). The decrease of the absorption peak at 330 nm revealed the reductive cleavage of **PTZ-P3** induced by H_2S, and was consistent with those of **PTZ-P1** and **PTZ-P2**. As shown in Fig. 3b, very weak emission of **PTZ-P3** (10 μM) was displayed in PBS buffer (pH = 7.4)/DMSO (1/2, 2% v/v PEG 400) without H_2S because of the strong ICT, but the emissions at 480 nm and 540 nm were both remarkably increased upon gradual addition of H_2S (0–700 μM). The enhanced emission at 480 nm was caused by **PTZCNSF** after reductive cleavage, which was consistent with those of **PTZ-P1** and **PTZ-P2**. However, heightening emission at 540 nm was related to the **BODIPY** moiety being released from **PTZ-P3**.

In the presence of H_2S, the ethylenic bond was reductively cleaved, so that optical properties of **PTZ-P4** were observed both

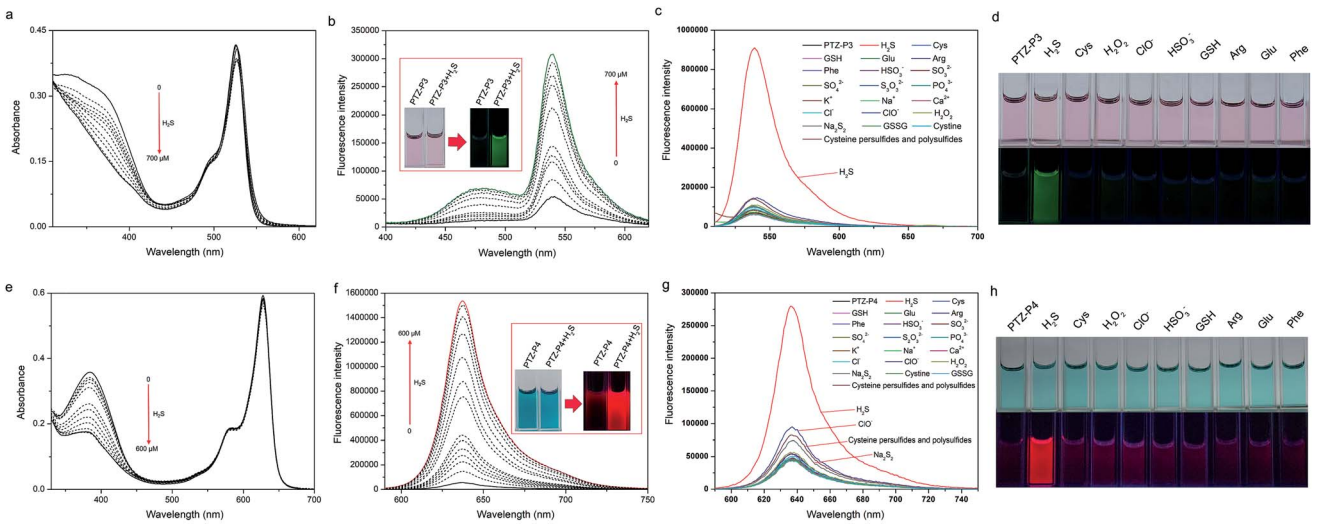

Fig. 3 (a and b) Absorption and fluorescence spectra of **PTZ-P3** (10 μM) in PBS buffer (pH = 7.4)/DMSO (1/2, 2% v/v PEG 400) with the addition of H_2S (0–700 μM), λ_{ex} = 330 nm. Inset in (b): photoimages of **PTZ-P3** with and without H_2S under daylight (left) and an ultraviolet lamp (365 nm; right). (c) The fluorescence spectra of **PTZ-P3** (10 μM) in the presence of H_2S (0.5 mM), Na_2S_2 (0.2 mM), cysteine persulfides and polysulfides (0.2 mM) and other analytes (0.5 mM) in PBS buffer (pH = 7.4)/DMSO (1/2, 2% v/v PEG 400), excitation: 500 nm. (d) Photoimages of **PTZ-P3** with H_2S (0.5 mM) and other analytes under daylight (above) and an ultraviolet lamp (365 nm, below). (e and f) Absorption and fluorescence spectra of **PTZ-P4** (10 μM) in PBS buffer (pH = 7.4)/DMSO (1/2, 2% v/v PEG 400) with the addition of H_2S (0–600 μM), λ_{ex} = 580 nm. Inset in (f): photoimages of **PTZ-P4** with and without H_2S under daylight (left) and an ultraviolet lamp (365 nm; right). (g) The fluorescence spectra of **PTZ-P4** (10 μM) in the presence of H_2S (0.5 mM), Na_2S_2 (0.2 mM), cysteine persulfides and polysulfides (0.2 mM) and other analytes (0.5 mM) in PBS buffer (pH = 7.4)/DMSO (1/2, 2% v/v PEG 400), excitation: 580 nm. (h) Photoimages of **PTZ-P4** with H_2S (0.5 mM) and other analytes under daylight (above) and an ultraviolet lamp (365 nm, below).

from **PTZCNSF** and **BOBPY**. Bearing this point in mind, the responses of absorption and fluorescence of **PTZ-P4** to H_2S were studied by gradual addition of NaHS solution into a PBS buffer (pH = 7.4)/DMSO (1/2, 2% v/v PEG 400) solution containing 10 μM probe. As illustrated in Fig. 3e, the absorption peaks of **PTZ-P4** at 384 nm were exhibited as decreasing, while the absorption peaks at 628 nm displayed almost no change after gradually adding H_2S (0–600 μM). As expected, the fluorescence spectra were consistent with **PTZ-P1** in the green region, but the red fluorescence was so strong that the weak green fluorescence was covered with the insignificant ratiometric change. As shown in Fig. 3f, the emission intensity at 638 nm (λ_{ex} = 580 nm) increased about 30-fold for **PTZ-P4** upon addition of 600 μM H_2S.

Selectivity of PTZ-P3 and PTZ-P4 to H_2S

The selectivity of the **PTZ-P3** and **PTZ-P4** towards H_2S was further identified. **PTZ-P3** and **PTZ-P4** (10 μM) were both treated respectively with various biologically relevant analytes in PBS buffer (pH = 7.4)/DMSO (1 : 2, 2% v/v PEG 400) for 10 min. As shown in Fig. 3c, d, g and h, the turn-on fluorescent responses of **PTZ-P3** and **PTZ-P4** are highly selective for H_2S *versus* biologically relevant thiols, reactive oxygen species (ROS) such as H_2O_2 and ClO^-, ions including K^+, Na^+, Ca^{2+}, HSO_3^-, SO_3^{2-}, SO_4^{2-} and $S_2O_3^{2-}$, and so on. Cysteine, cystine, glutathione, Na_2S_2, and cysteine persulfides and polysulfides[24] induced very little increase of fluorescence intensity. Therefore, both **PTZ-P3** and **PTZ-P4** showed high selectivity for H_2S.

Imaging exogenous H_2S in living cells

After developing these probes based on the novel reductive cleavage of C=C bonds, we explored the applications of **PTZ-P4** in monitoring H_2S under physiological conditions. The cytotoxicity of **PTZ-P4** was evaluated in HeLa cells using a MTT assay.

As described in Fig. S7†, **PTZ-P4** exhibited relatively low toxicity towards HeLa cells with good viability. Putting **PTZ-P4** into practice, exogenous H_2S was detected in living HeLa cells. Firstly, HeLa cells were exposed to 20 μM **PTZ-P4** for 5 h, then NaHS solution was used as the exogenous H_2S source at 100 μM, incubating with cells for another 3 h. Compared with cells treated with only **PTZ-P4**, there was obvious green and red fluorescence in cells treated with both H_2S and **PTZ-P4** (Fig. 4).

Imaging endogenous H_2S in living *C. elegans*

Endogenous H_2S mainly originates from sulfur-containing amino acids metabolized by at least three enzymes: cystathionine β-synthase (CBS), cystathionine γ-lyase (CSE) and 3-mercaptopyruvate sulfur transferase (3-MST).[25] *C. elegans* is an excellent *in vivo* model system for monitoring physiological H_2S with clear molecular mechanisms of H_2S action.[26,27] Specifically, it has been shown that the germline-deficient *glp-1* (*e2144*) mutants displayed increasing production of endogenous H_2S, while the deletion mutation in *cth-1*, the gene encoding the H_2S synthesizing enzyme cystathionine γ-lyase, resulted in down-regulated H_2S levels.[27–30] To further understand the features of

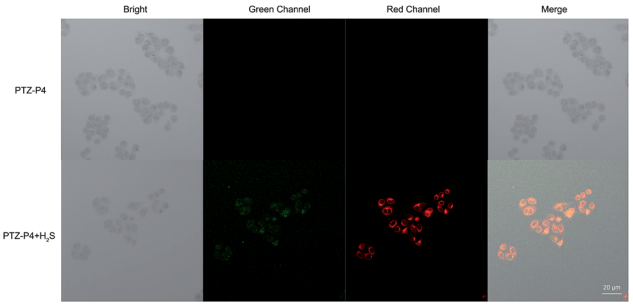

Fig. 4 Confocal images of exogenous H_2S in HeLa cells without (top) and with (bottom) 100 μM H_2S in the presence of 20 μM **PTZ-P4**. Scale bar: 20 μm.

PTZ-P4, *in vivo* imaging was employed to visualize endogenous H_2S in *C. elegans*. Concentrations of **PTZ-P4** and time periods used for feeding were titrated to ensure enough **PTZ-P4** absorption and metabolism without significant biotoxicity (data not shown). In living *C. elegans*, **PTZ-P4** should be absorbed, distributed, metabolized and excreted, and so 200 μM **PTZ-P4** was used to make sure that there was enough **PTZ-P4** in *C. elegans* for *in vivo* imaging. As a representative example shown in Fig. 5a, both green and red fluorescence were observed in wild-type N2 worms after being fed with 200 μM **PTZ-P4** for 48 h. Additionally, H_2S was mainly accumulated in intestinal cells, predominantly in the cytoplasm, and in apical membranes as well (Fig. 5a and data not shown).

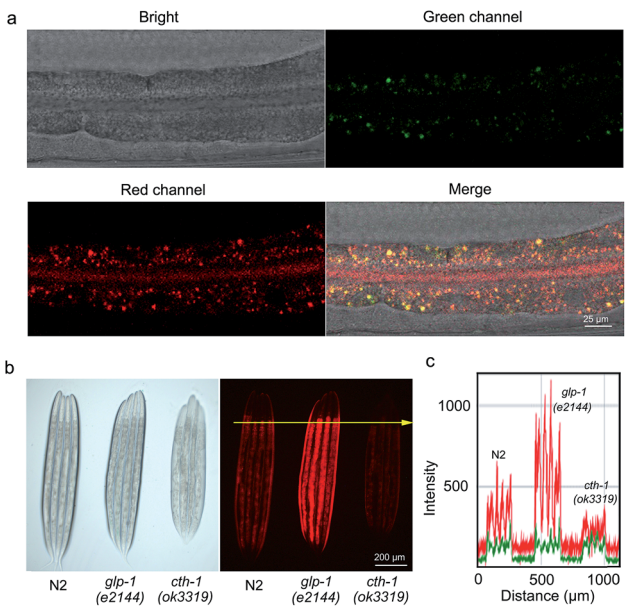

Fig. 5 (a) Confocal images captured the H_2S distribution in wild type N2 with 200 μM **PTZ-P4**; the scale bar was 25 μm. (b) Fluorescence images of endogenous H_2S in wild type N2, germline-deficient *glp-1* (*e2144*) mutants and *cth-1* (*ok3319*) mutants incubated with 200 μM **PTZ-P4**. Normal, elevated and reduced endogenous H_2S levels are shown from left to right; the scale bar was 200 μm. (c) Fluorescence intensities were measured along a line crossing the anterior of the intestine.

Consistent with changes of H_2S levels in different strains, the red fluorescence intensity of *glp-1* (*e2144*) mutants was obviously stronger than that in wild-type N2 worms, while *cth-1* (*ok3319*) mutants exhibited notably weaker red fluorescence compared with wild-type N2 worms (Fig. 5b and c). This result suggested that red fluorescence signals could be clearly captured with significant changes and successfully reflected different H_2S levels under different physiological conditions. Of note, differences in green fluorescence among different strains were also detected, albeit to a less appreciable level (Fig. 5c), due to the weak absorbance of **PTZCNSF** at 405 nm (the excitation wavelength of the fluorescence microscope). Altogether, these results provided compelling evidence that **PTZ-P4** is highly sensitive and selective with dual fluorescent colors to detect endogenous H_2S in living systems and can be used as a potential probe for *in vivo* imaging of endogenous H_2S.

A significant bottleneck in detecting H_2S is the effective imaging of endogenous H_2S *in vivo*, a problem that restrains the biological applications. In the current study, the dual-color fluorescent probe **PTZ-P4** showed high selectivity for H_2S *versus* cysteine or glutathione. It also demonstrated a good response concurrently with the application in different strains of *C. elegans*, showing distinct differences in brightness for wild type N2, *glp-1* (*e2144*) and *cth-1* (*ok3319*) mutants.

Conclusions

In summary, we have discovered H_2S-mediated reductive cleavage of C=C bonds under mild conditions, which was successful as a new strategy to design fluorescent probes for effective detecting of H_2S. Of these probes, **PTZ-P4** displayed dual-color turn-on fluorescence upon *in vivo* sensing of endogenous H_2S in different strains of *C. elegans*, showing distinct differences in brightness for wild type N2, *glp-1* (*e2144*) and *cth-1* (*ok3319*) mutants. As far as we know, this is the first report that H_2S can reductively cleave C=C bonds under mild conditions. As C=C bonds are actively involved in various organic reactions, the discovery of this reductive cleavage of C=C is anticipated to be valuable not only for the development of C=C bonds in synthetic chemistry and theoretical studies, but also for the design of new fluorescent H_2S probes for bioimaging and sensing applications.

Conflicts of interest

The authors declare no competing financial interest.

Acknowledgements

This work was supported by the Macao Science and Technology Development Fund under Grant No.: 052/2015/A2, 082/2016/A2, and 019/2017/AMJ to X.Z, and 060/2015/A2, 018/2017/AMJ; 050/2018/A2 to H.Z; the Research Grant of University of Macau No.: MYRG2016-00058-FHS and MYRG2017-00066-FHS to X.Z, MYRG2016-00066-FHS and MYRG2017-00082-FHS to H.Z. We thank the *C. elegans* Genetic Center, funded by NIH Office of Research Infrastructure Programs (P40 OD010440), for strains.

Notes and references

1 A. Chatupheeraphat, H. H. Liao, W. Srimontree, L. Guo, Y. Minenkov, A. Poater, L. Cavallo and M. Rueping, *J. Am. Chem. Soc.*, 2018, **140**, 3724–3735.
2 R. R. Gu, K. Flidrova and J. M. Lehn, *J. Am. Chem. Soc.*, 2018, **140**, 5560–5568.
3 M. Daini and M. Suginome, *J. Am. Chem. Soc.*, 2011, **133**, 4758–4761.
4 J. Dey, A. C. O'Donoghue and R. A. M. O'Ferrall, *J. Am. Chem. Soc.*, 2002, **124**, 8561–8574.
5 K. Fuji, T. Kawabata, M. Node and E. Fujita, *Tetrahedron Lett.*, 1981, **22**, 875–878.
6 K. Fuji, T. Kawabata, M. Node and E. Fujita, *J. Org. Chem.*, 1984, **49**, 3214–3216.
7 K. Chen, H. Li, Z. Q. Lei, Y. Li, W. H. Ye, L. S. Zhang, J. Sun and Z. J. Shi, *Angew. Chem., Int. Ed.*, 2012, **51**, 1–6.
8 A. V. Bogdanov, A. V. Petrova, D. B. Krivolapov and V. F. Mironov, *Tetrahedron Lett.*, 2014, **55**, 6615–6618.
9 V. S. Lin and C. J. Chang, *Curr. Opin. Chem. Biol.*, 2012, **16**, 595–601.
10 Y. C. Chen, C. C. Zhu, Z. H. Yang, J. J. Chen, Y. F. He, Y. Jiao, W. J. He, L. Qiu, J. J. Cen and Z. J. Guo, *Angew. Chem., Int. Ed.*, 2013, **125**, 1732–1735.
11 J. Liu, Y. Q. Sun, J. Y. Zhang, T. Yang, J. B. Cao, L. S. Zhang and W. Guo, *Chem.–Eur. J.*, 2013, **19**, 4717–4722.
12 V. S. Lin, W. Chen, M. Xian and C. J. Chang, *Chem. Soc. Rev.*, 2015, **44**, 4596–4618.
13 X. Feng, T. Zhang, J. T. Liu, J. Y. Miao and B. X. Zhao, *Chem. Commun.*, 2016, **52**, 3131–3134.
14 R. Wang, F. B. Yu, L. X. Chen, H. Chen, L. J. Wang and W. W. Zhang, *Chem. Commun.*, 2012, **48**, 11757–11759.
15 W. Chen, C. R. Liu, B. Peng, Y. Zhao, A. Pacheco and M. Xian, *Chem. Sci.*, 2013, **4**, 2892–2896.
16 M. Gao, F. B. Yu, H. Chen and L. X. Chen, *Anal. Chem.*, 2015, **87**, 3631–3638.
17 Y. Huang, F. B. Yu, J. C. Wang and L. X. Chen, *Anal. Chem.*, 2016, **88**, 4122–4129.
18 R. Y. Lai, X. X. Kong, S. A. Jenekhe and A. J. Bard, *J. Am. Chem. Soc.*, 2003, **125**, 12631–12639.
19 W. G. Yang, S. H. Yang, Q. R. Guo, T. Zhang, K. Y. Wu and Y. H. Hu, *Sens. Actuators, B*, 2015, **213**, 404–408.
20 K. M. Vengaian, C. D. Britto, K. Sekar, G. Sivaraman and S. Singaravadivel, *Sens. Actuators, B*, 2016, **235**, 232–240.
21 Z. S. Huang, H. Meier and D. R. Cao, *J. Mater. Chem. C*, 2016, **4**, 2404–2426.
22 M. Frank, J. Ahrens, I. Bejenke, M. Krick, D. Schwarzer and G. H. Clever, *J. Am. Chem. Soc.*, 2016, **138**, 8279–8287.
23 N. Chen, W. J. Zhang, S. Chen, Q. H. Wu, C. J. Yu, Y. Wei, Y. K. Xu, E. H. Hao and L. J. Jiao, *Org. Lett.*, 2017, **19**, 2026–2029.
24 S. Koike, S. Nishimoto and Y. Ogasawara, *Redox Biol.*, 2017, **12**, 530–539.

25 J. Y. Zhang, Y. P. Ding, Z. Wang, Y. Kong, R. Gao and G. Chen, *Med. Gas Res.*, 2017, **7**, 113–119.
26 D. L. Miller and M. B. Roth, *Proc. Natl. Acad. Sci. U. S. A.*, 2007, **104**, 20618–20622.
27 Y. H. Wei and C. Kenyon, *Proc. Natl. Acad. Sci. U. S. A.*, 2016, **113**, 2832–2841.
28 N. Arantes-Oliveira, J. Apfeld, A. Dillin and C. Kenyon, *Science*, 2002, **295**, 502–505.
29 J. R. Berman and C. Kenyon, *Cell*, 2006, **124**, 1055–1068.
30 B. Qabazard, L. Li, J. Gruber, M. T. Peh and L. F. Ng, *Antioxid. Redox Signaling*, 2014, **20**, 2621–2630.